Journal of Organometallic Chemistry 904 (2019) 121003

Contents lists available at ScienceDirect

Journal of Organometallic Chemistry

journal homepage: www.elsevier.com/locate/jorganchem

Computational and experimental assessment on the nonlinear optical properties of platinum(II) arylacetylides with donor-acceptor structures

Fengli Wei [a], Xuewei Huang [a], Zhaoxun Lian [b, ***], Yanyan Zhu [a, **], Fengqi Guo [a, *]

[a] College of Chemistry, Zhengzhou University, Zhengzhou, Henan, 450001, PR China
[b] School of Chemistry and Chemical Engineering, Henan Institute of Science and Technology, Xinxiang, Henan, 453003, PR China

ARTICLE INFO

Article history:
Received 17 August 2019
Received in revised form
22 October 2019
Accepted 23 October 2019
Available online 24 October 2019

Keywords:
Nonlinear optical properties
Platinum acetylides
Z-scan
TD-DFT
Relationship between the structure and the properties

ABSTRACT

The nonlinear optical properties of eight platinum acetylides with donor-acceptor structures were investigated via computational and experimental methods, and the relationship between the structures and the properties was discussed deeply based on the computational and experimental results. The contributions of all the atoms to the electronic density of HOMO and LUMO of the platinum acetylide complexes were calculated using the time-dependent density functional theory (TD-DFT) with exchange correlation function B3LYP, and the first-order hyperpolarizabilities of them were also calculated in the same conditions. Z-scan results indicated that the electronic asymmetric property is an important factor affected the nonlinear optical properties, and the nonlinear absorption properties of a molecule can be enhanced by enlarging the conjugate length of the molecule. The nonlinear optical property of the molecules with two electron donor groups at both sides of their skeletons are better than that of the molecules with two electron withdrawing groups. Enlarging the conjugated area in the center of the molecule was disadvantageous to the nonlinear absorption property of the molecule, and the large contribution of the heavy-atom to the electronic density of HOMO of a molecule doesn't mean the better nonlinear absorption property. The large values of σ_e/σ_g and the short fluorescence lifetimes of the complexes infer that the nonlinear absorption behavior of the titles complexes should be originated reverse saturable absorption.

1. Introduction

Nonlinear optical materials have attracted considerable attention in the past decades because of their applications in optical modulation, frequency conversion, data storage, optical power limiting and so on [1–4]. Several kinds of materials with special nonlinear optical properties, such as inorganic semiconductors, macrocyclic metal complexes, fullerene, conjugated polymers, organic molecules, and nanocrystals, have been investigated detailedly, and different mechanisms corresponding to those materials have been reported [5–10]. It has been testified that the organic small molecules with donor (D)-acceptor (A) structures generally have excellent two photon absorption properties, and their two-photon absorption cross sections can be increased by extending the molecular conjugated system and increasing the electronic asymmetry via using more potent donating or accepting moieties [11]. In addition, it also has been reported that the molecules containing heavy atoms and rigid structure generally have good reverse saturable absorption property due to the large intersystem crossing coefficient from the first singlet excited state to the first triplet excited state [12–14]. Although all these kind of materials still have not been applicated in reality, the conclusions of the previous work are helpful for designing the materials with large nonlinear optical properties.

Platinum aromatic acetylides as a new type functional material have been studied intensively in recent years [15–17]. The heavy metallic ion and the rigid C≡C triple bond-containing π conjugated system confer these organometallic oligomers great unique properties, especially the great nonlinear optical property [18,19]. Several groups, including ours, have proved that platinum aromatic

* Corresponding author.
** Corresponding author.
*** Corresponding author.
E-mail addresses: zhxalian@163.com (Z. Lian), zhuyan@zzu.edu.cn (Y. Zhu), fqguo@zzu.edu.cn (F. Guo).

https://doi.org/10.1016/j.jorganchem.2019.121003
0022-328X/

acetylides exhibit high linear transmission and strong reverse saturable absorption from visible to infrared spectral region because of the spin-orbit coupling interaction between the d orbitals of the heavy metal Pt(II) ion and the large π-conjugated system [14,20–22]. The two-photon absorption phenomenon of several platinum aromatic acetylides has also been reported recently, and the enhanced nonlinear optical absorption based on the absorption from both the singlet and triplet states also have been confirmed [23–25]. However, the detailed relationship between the structure, the two-photon absorption and the excited state absorption of the organic molecules are still not discussed clearly. Especially, whether the two-photon absorption and the excited state absorption of an organic molecule restrain each other is also not discussed deeply up to now. So it is necessary and important to address these questions for design nonlinear optical materials.

In order to address the questions, eight symmetric or unsymmetrical platinum aromatic acetylides with donor-acceptor structures, as shown in Scheme 1, have been designed and synthesized. The synthetic processes, photophysical properties and the first-order hyperpolarizabilities determined by the solvatochromic method have been reported in the previous paper [26]. The absorption of all the title platinum acetylides above 450 nm is very weak, which provides a wide observation window for the application in optical power limiter. The low fluorescent quantum yields and detectable room temperature phosphorescence indicate that the complexes containing Pt(II) have pretty high system-cross quantum yields because of the spin-orbit coupling between the d orbitals of the Pt(II) and the large π-conjugated system, which confers that this kind of platinum aromatic acetylides are promising nonlinear optical materials. In this paper, the nonlinear optical properties were investigated via computational and experimental methods, and the relationship between the structure and the properties was discussed deeply based on the computational and experimental results.

2. Z-scan experiments

The Z-scan technique was used to evaluate the third-order nonlinear optical susceptibilities of the title compounds in DMF, and the Z-scan experimental set-up is shown schematically in Fig. 1 [27–29]. The initial laser beam is divided into two beams by a beam splitter BS1 after passing through an energy attenuator, and the reflected part is collected by detector D1 to monitor the fluctuation of incident pulse energy. The laser beam passing through BS1 is tightly focused and then is divided into two parts by the beam splitter BS2 behind the focus, and the reflected part is all received by the detector D2, while the transmitted part is received by the detector D3 after passing through an aperture, the output laser energy was noted using Laser Probe Rj-7620 energy ratio-meter with two pyroelectric detectors. The solution of the sample was placed in a 2-mm thick quartz cell near the focus. The energies of the laser beams after passing through the sample with and without aperture were monitored when the sample moved through the

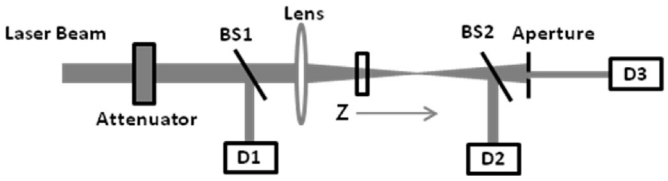

Fig. 1. Experimental setup of the single beam Z-scan.

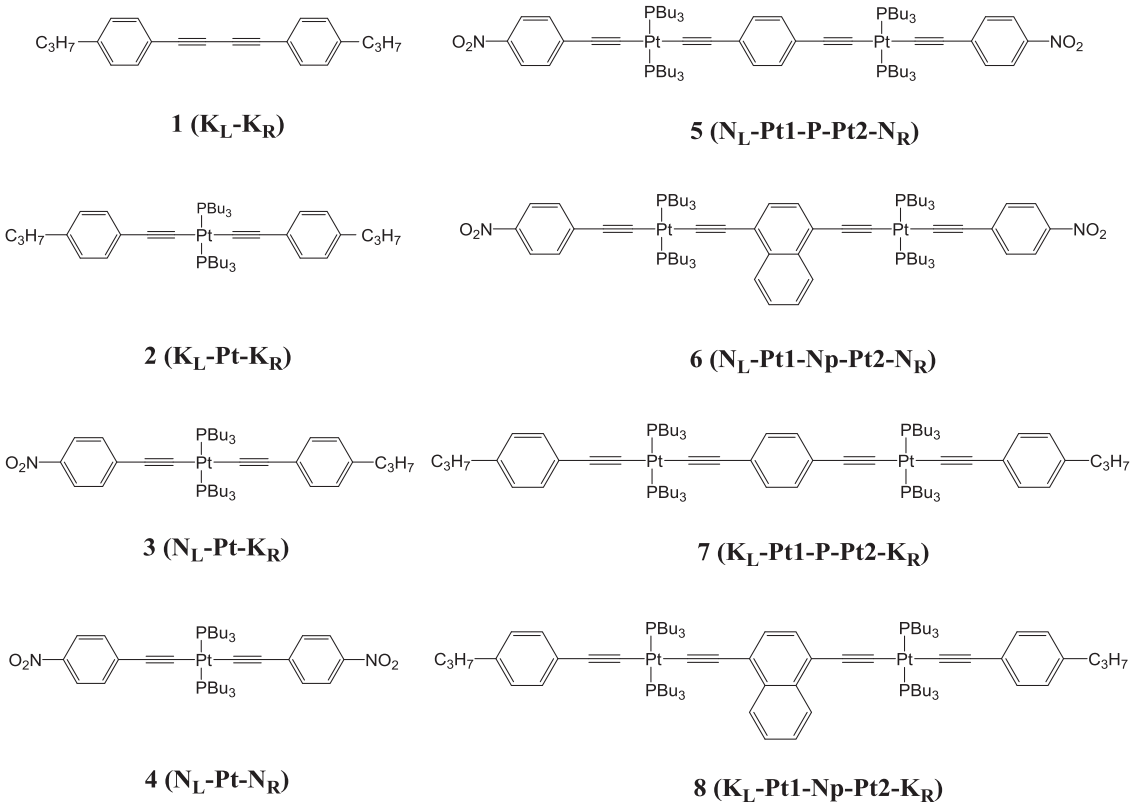

Scheme 1. Structures of the synthesized platinum aromatic acetylides with donor-acceptor structures.

focal plane along the Z-axis. A Q-switched, frequency doubled Nd:YAG laser (Beamtech Optronics Co., Ltd., Dawa-200) producing 532 nm laser beam with 7ns pulse width and repetition rate of 10 Hz was used as the laser resource, and the output of the laser beam has a nearly Gaussian intensity profile. The Gaussian laser beam was focused by a lens with 25 cm focal length. The waist radius of the focused beam spot was found to be 33 μm (ω_0), the corresponding Rayleigh length, calculated using the formula $Z_0 = \pi\omega_0^2/\lambda$, was found to be 6.43 mm. The sample thickness is less than the Rayleigh length; hence the thin sample approximation is valid [30].

All the platinum aromatic acetylides were dissolved in DMF with concentration of 1 x 10^{-3} mol/L. The absorption cross-sections of the excited state (σ_e) of the samples can be obtained base on the open aperture Z-scan experimental data and the nonlinear absorption coefficients (β) can be also calculated according to the literature method [29,31].

The normalized transmittance of the open aperture Z-scan experiments is given by the following equation:

$$T_{(Z)} = \left[\frac{1+x^2}{q_0}\right]\ln\left[1+\frac{q_0}{1+x^2}\right] \quad (1)$$

where $x = Z/Z_0$, Z is the distance from the sample to the focus. q_0 is a free factor defined as:

$$q_0 = \frac{\alpha\delta_{ex}F_0L_{eff}}{Zh\omega} \quad (2)$$

In which ω is the angular frequency of the laser. F_0 is the on-axis fluence at the focus, which is related to the incident laser energy E_{total}, ω_0 is the beam waist, $L_{eff} = (1\text{-}e^{-\alpha L})/\alpha$, α is the linear absorption coefficient of the sample and L is the length of the sample.

The linear absorption coefficient α of the sample can be obtained from the equation, $\alpha = 10^{-3}\sigma_g N_A C$, where C is the molar concentration of the sample, N_A is the Avogadro constant and σ_g is the absorption cross-section area of the ground state of the sample. The value of q_0 can be obtained by fitting the experimental data of the open aperture Z-scan with Eq. (1), and then the absorption cross-section area of the excited state σ_e of the target molecule can be calculated out according Eq. (2). Finally the nonlinear absorption coefficient β can be calculated out based on the value of σ_e.

3. Results and discussion

3.1. Quantum calculation of electronic orbital properties

In order to investigate the relationship between the structure and properties of the title compounds deeply, the electronic properties of them were calculated theoretically using the Gaussian 09 program package [32]. To verify the most suitable method for the calculation, the geometry and electronic properties of **2** in chloroform were optimized and calculated using the time-dependent functional theory (TD-DFT) method, which is a reliable tool for calculating the excited states for 3d transition metal-containing compounds with the open-shell electrons [33], with three different exchange correlation functionals, B3LYP, BHandHLYP and ωB97, respectively. The mixed basis set 6-311G++ (2d, 2p) for C, N, O, P, H atoms and the core potential basis set of LanL2DZ for Pt atom were selected. LanL2DZ is a relativistic effective core potential basis set for the calculation of transition metals [34–37]. The UV–vis absorption spectra based on the calculating results with those three different exchange correlation functions were simulated with the SWizard [38]. The simulated UV–Vis absorption spectra and the experimental absorption spectrum of **2** were presented in Fig. 2. It is obvious that the absorption spectrum of **2** calculated using B3LYP was more consistent with the experimental spectrum than those calculated using ωB97 and BHandHLYP. So the geometries and the electronic properties of the other title compounds were all calculated using TD-DFT method with B3LYP exchange correlation functional and all the simulated absorption spectra of them were showed in Fig. S1. Then the resulted files containing the information of the ground and excited-state electronic structures of the title compounds were used as the input files to analyze the orbitals of the title compounds using DFT/B3LYP method.

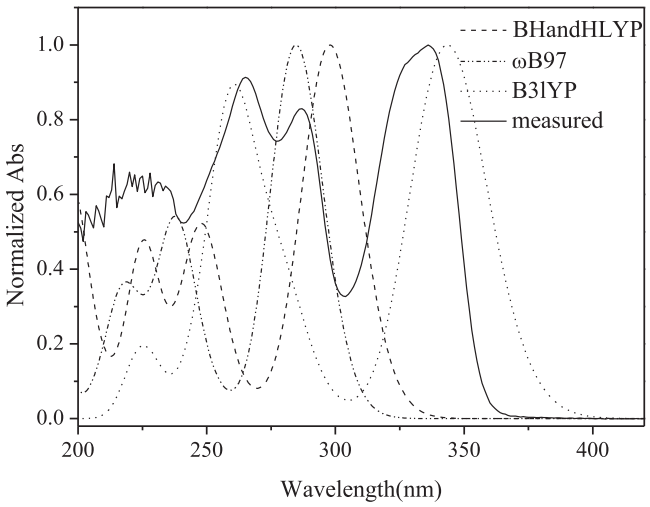

Fig. 2. The measured and calculated UV–vis absorption spectra of **2** in chloroform using DFT method with BHandHLYP, ωB97, B3LYP, exchange correlation functional, respectively.

The computed energy gaps (Eg), the oscillator strengths (f) of the electronic transitions and the absorption maximums between the ground state (S_0) and the first singlet excited state (S_1), as well as the corresponding experimental data of the title complexes were listed in Table 1. The calculated frontier molecular orbital energy levels and main transition processes of the title compounds (four occupied and four unoccupied orbitals, and energy gaps between HOMO and LUMO) are also shown in Fig. 3. It can be seen from Fig. 3 and Table 1 that the electronic asymmetry of the molecule affects the properties of molecular orbitals and transition characters greatly. The calculated absorption spectra of all the compounds, as shown in Fig. 2 and Fig. S1, exhibit intense absorption bands from 300 nm to 420 nm, which can be assigned to the π-π* transition and partly MLCT (metal-to-ligand charge transfer transition, d_M-π_L^*) and moderate intense absorption bands from 200 nm to 300 nm, which were assigned to $\pi \rightarrow \pi^*$ transition of the aryl rings, this is consistent to the results reported in previous literatures and the experimental results [26,39]. For compound **4**, **5** and **6**, the HOMOs and the LUMOs of them should be degenerated orbitals according to the calculated frontier molecular orbital energy levels showed in Fig. 3. The calculated spectroscopy information of the title compounds is pretty consistent with the experimental results in view of the large molecular quantity of the title compounds [26]. The difference of the absorption maximum between the calculated and experimental results of **1,** in which no Pt atom is contained in the structure, was 45 nm. This large difference should be because of the calculation method TD-DFT, which is a reliable tool for calculating the excited states for 3d transition metal-containing compounds with the open-shell electrons. Comparison of the calculated absorption spectra of **2**, **7** and **8**, in which two electron donors were

Table 1
The measured and calculated absorption maxima, the calculated oscillator strengths (f) and the energy gaps between HOMO and LUMO (eV) of the title compounds.

Complex	Abs Maximum (nm)	TD-DFT	E_g/eV	*f*	Transition characteristics	
1	315	361	3.44	1.4973	HOMO - > LUMO	94%
2	336	343	3.61	0.9844	HOMO- > LUMO	95%
3	387	386	3.21	0.6765	HOMO-2- > LUMO	97%
4	390	416	2.98	1.0158	HOMO- > LUMO HOMO-1- > LUMO	59%
						38%
5	399	397	3.13	1.0925	HOMO-3- > LUMO+1	79%
					HOMO-2- > LUMO+1	13%
6	396	408	3.04	2.2570	HOMO- > LUMO+2	42%
					HOMO-3- > LUMO+1	18%
7	362	356	3.48	1.9777	HOMO- > LUMO	92%
8	390	406	3.05	1.4204	HOMO- > LUMO	97%

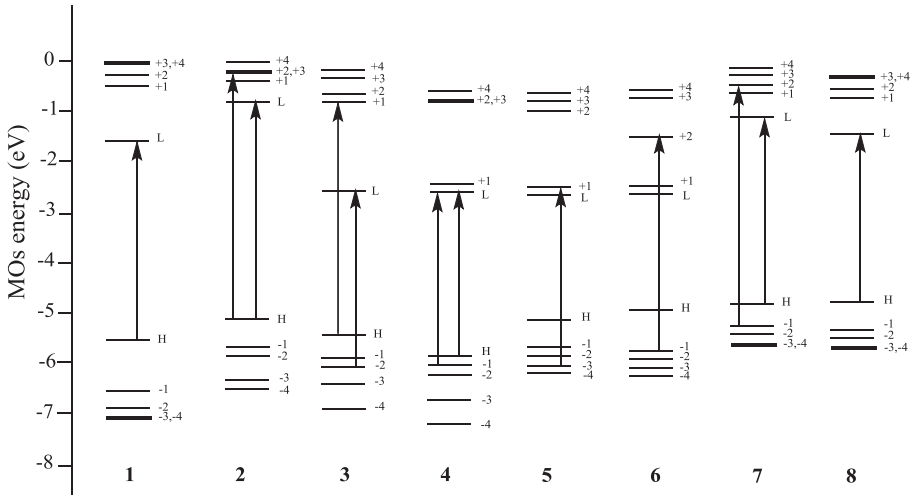

Fig. 3. Calculated frontier orbital energy levels and the main transition processes of the title compounds.

connected to the two sides of the molecules, inferred that the increasing of the conjugated system of the molecule induced red shift in the absorption maxima. However, for compounds **4**, **5** and **6**, in which two electron acceptors were connected to the two sides of the molecules, there is no obvious red shift in the absorption maxima. It can also be concluded that replacing the electron donor by electron acceptor induces the absorption maxima red shift by comparison of the absorption spectra of **2**, **3** and **4**. The absorption spectra of **5**, **7**, **6** and **8** suggested the same conclusion.

The electronic density distribution of HOMO and LUMO were shown in Fig. 4, and the contributions of all the fragments of the title compounds to the electronic density of HOMO and LUMO are listed in Table 2. The measured and calculated energy levels, as well as the energy gaps (E_g) between HOMO and LUMO, were also listed in Table 3. It can be seen from Fig. 4 that the title platinum aromatic acetylides with donor-acceptor structure keep the conjugated system after the insertion of Pt(II) ion into the skeleton of an organic molecule and the electron transfer process could occur by passing through the metal ions. The energy levels of the HOMO and LUMO of the title compounds decrease when the electron donor is replaced by an electron acceptor, and the energy intervals between HOMO and LUMO decrease at the same time. In addition, the insertion of the central aryl groups increases the energy levels of HOMO and LUMO and makes the electronic density of HOMO more localized on the conjugated ligands with less contribution of the metal d_π. These calculational results are consistent with the literature and measured data [26]. It is well known that the second-order NLO response is closely related to charge transfer, and the charge transfer behavior of these kinds of compounds is dominated by the asymmetry of the molecular skeleton, which makes it possible to study the ffect of the insertion of heavy metal ions and the donor-acceptor structure on the nonlinear optical properties of the organic molecules. In order to investigate the charge transfer properties of the title compounds, the charge density difference maps corresponding to the electronic transitions of them were calculated and showed in Fig. S2. It is clear that the charge flows from electron-poor acceptor moiety to the electron-rich donor part for all the title compounds, the intramolecular charge transfer occurred clearly. This result is consistent with the electronic density distribution of HOMO and LUMO shown in Fig. 4.

3.2. Calculation of the first-order hyperpolarizabilities

To investigate the nonlinear optical behavior of the title molecules in microscopic view, the first-order hyperpolarizability (β) tensors of them were calculated by defining the mass center of the molecules as the origin of the Cartesian coordinate system, with which the first-order hyperpolarizability can be depicted by a $3 \times 3 \times 3$ matrix [40]. The 27 tensors of the first-order hyperpolarizability in $3 \times 3 \times 3$ matrix can be minimized to 10 components due to the Kleinman symmetry [41]. The 10 components of the first -order hyperpolarizabilities, β_{xxx}, β_{xxy}, β_{xyy}, β_{yyy}, β_{xxz}, β_{xyz}, β_{yyz}, β_{xzz}, β_{yzz} and β_{zzz} of the title complexes, were calculated out and listed in Table 4. The magnitudes of x, y and z tensors of the first-order hyperpolarizability can be calculated according to the following equation (3):

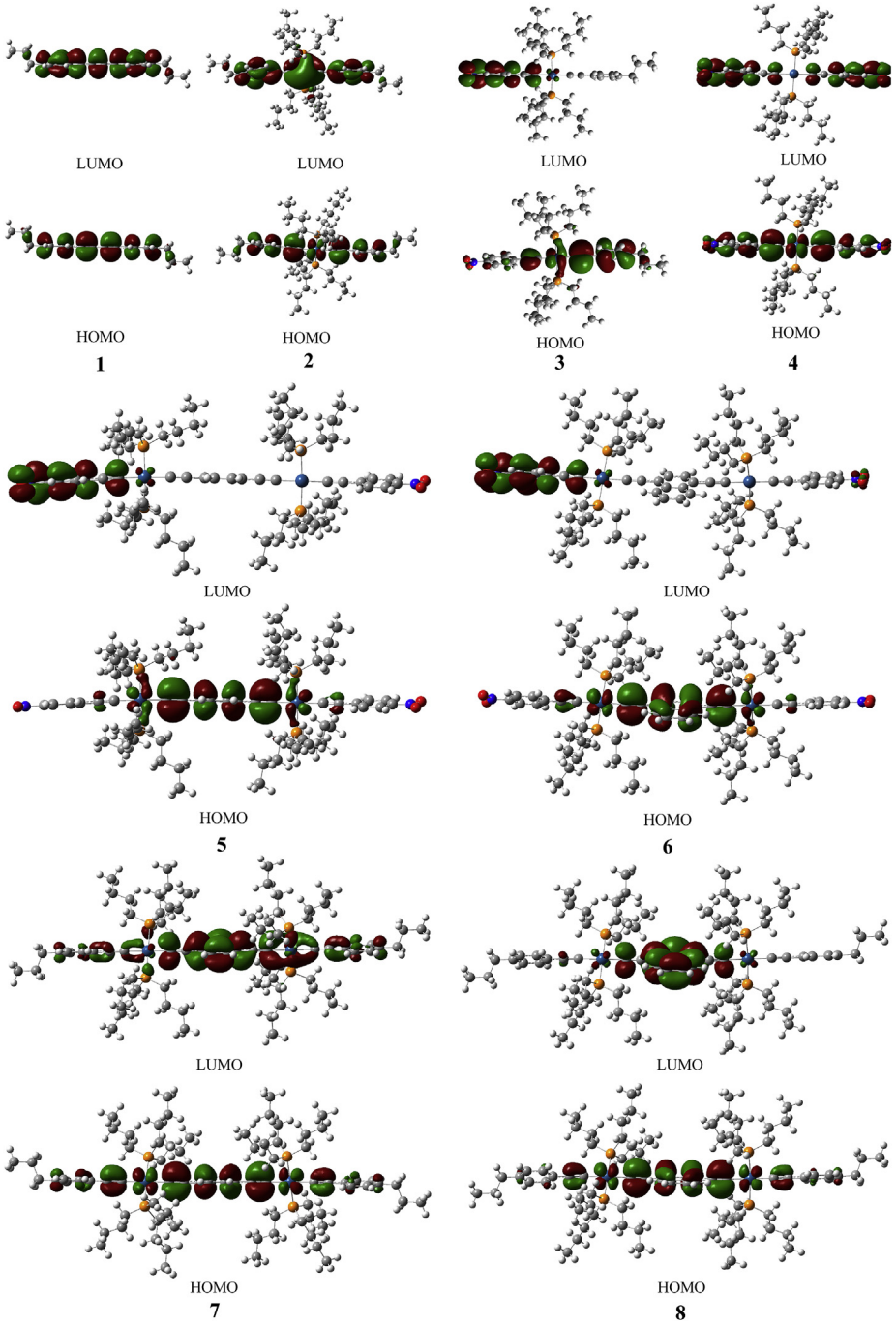

Fig. 4. Electronic density distribution of HOMO and LUMO of the title compounds.

$$\beta_i = 3/5\ (\beta_{iii} + \beta_{ijj} + \beta_{ikk})\ i, j, k = x, y, z \quad (3)$$

Then the magnitude of the first-order hyper polarizability can be estimated according to equation (4), and the calculated first-order hyperpolaizabilities obtained from B3LYP/6-311G++(2d, 2p) were also enumerated in Table 4.

$$\beta=(\beta_x^2 + \beta_y^2 + \beta_z^2)^{1/2} \quad (4)$$

It can be seen from Table 4 that the first-order hyperpolarizability of **1** is far smaller than that of the others, which should be because that the mechanism of the nonlinear optical property of title molecules is ascribed to the reverse saturable absorption for the nanosecond laser, while compound **1** does not contain heavy metallic ions in the skeleton and also is the smallest conjugated system that are not beneficial to improve β [42]. The first-order hyperpolarizability of **3**, in which an electron donor and an electron acceptor are connected to the two sides of its skeleton respectively, is the largest one compared to that of **2** and **4**. It indicated that the electronic asymmetric property affected the nonlinear optical properties greatly, and it is consistent with the earlier reported results [43]. The first-order hyperpolarizabilities of **4, 5, 6** with two electron acceptors at both sides of their skeletons are larger than that of **2**, **7** and **8** with two electron withdrawing

Table 2
Contributions of all the fragments to the electronic density of the HOMO and LUMO of the title compounds.

HOMO		1	2	3	4	LUMO	1	2	3	4
Pt%		–	32.9	24.9	36.1	Pt%	–	13.6	1.49	0.53
K_L%		46.7	31.5	–	–	K_L%	45.5	34.0	–	–
K_R%		46.7	29.4	39.0	–	K_R%	45.5	26.4	0.2	–
N_L%		–	–	7.4	27.2	N_L%	–	–	96.8	46.9
N_R%		–	–	–	34.2	N_R%	–	–	–	49.7
HOMO		**5**	**6**	**7**	**8**	LUMO	**5**	**6**	**7**	**8**
Pt1%		9.59	11.27	13.05	13.02	Pt1%	1.45	1.43	5.46	3.54
Pt2%		8.99	7.29	15.54	9.29	Pt2%	0.002	0.02	5.96	1.86
N_L%		48.39	16.87	17.39	16.56	N_L%	64.3	90.2	10.65	6.39
P%	28.98	–	22.06	–	P%	0.09	–	42.48	–	
Np%	–	39.35	–	34.96	Np%	–	0.19	–	71.91	
N_R%	18.92	15.55	18.21	15.44	N_R%	0.23	1.84	11.41	5.98	

"——" means that the contribution is negligible small.

Table 3
Calculated energy levels of HOMO and LUMO, the energy gaps between HOMO and LUMO of the title complexes.

Compound	1	2	3	4	5	6	7	8
LUMO/eV	−1.66	−0.97	−2.62	−2.69	−2.63	−2.61	−1.02	−1.46
HOMO/eV	−5.60	−5.17	−5.43	−5.93	−5.17	−5.04	−4.99	−4.87
ΔE/eV	3.94	4.20	2.81	3.24	2.54	2.43	3.97	3.41
[a]ΔE/eV	3.55	3.47	2.66	2.73	2.64	2.62	3.18	2.87

[a] Measured energy gaps between HOMO and LUMO of the title complexes.

groups at both sides of their skeletons, which inferred that the nonlinear optical properties of the molecules with two electron acceptors at both sides of their skeletons are better than that of the molecules with two electron donor groups at both sides of their skeletons. To enlarge the conjugate length of the molecules could enhance the nonlinear optical properties of the molecules, while to enlarge the conjugated area in the center of the molecule doesn't affect the first-order hyperpolarizability greatly. The first-order hyperpolarizability of **3** is far larger than that of 5, **6**, **7** and 8, which inferred that the electronic asymmetry of a molecule affect the nonlinear optical property heavier than the conjugated length of the molecule.

3.3. Z-scan studies

The nonlinear absorption properties of **1**–**8** in DMF were measured using the open aperture Z-scan technology, a laser with 532 nm wavelength and 7ns pulse-width was used as the laser source. The open aperture Z-scan traces and the theoretical fitting curves of the compounds according to Equation (1) were shown in Fig. 5, and all the effective absorption cross-sections of the excited states of the compounds obtained by fitting the experimental data were listed in Table 5. In addition, the calculated ground state absorption cross-sections, the ratios of σ_e/σ_g and the effectively nonlinear absorption coefficients (β) were also listed in Table 5.

It can be seen from Fig. 5 that the normalized transmittance decreased with the increasing of the on-axis laser intensity and reached to minimum values when the samples were at the focus position of the lens, which inferred a nonlinear absorption behavior in view of the weak linear absorption of the title compounds at 532 nm [44]. The pulse width of the laser used in our experiments is 7 ns, which is much longer than the fluorescence lifetimes of the compounds [26], so the nonlinear absorption behavior should be originated from reverse saturable absorption (RSA).

RSA behavior is only occurred when the excited singlet state absorption cross-section (σ_e) is greater than the ground state absorption cross-section (σ_g) of a compound. It is quite obvious that the excited-state absorption cross-sections of **1**–**8** are larger than those of the ground states from the data listed in Table 5, it indicates that attributing the nonlinear absorption of the compounds to RSA is reasonable. The ratio of σ_e/σ_g and the effectively nonlinear absorption coefficients (β) are the favourite parameters to describe the overall nonlinear absorption properties. Compound **3** with an electron withdrawing $-NO_2$ group and an electron pushing $-CH_3$ group, respectively, on the two sides of the molecule has the largest σ_e/σ_g value of 3.1 and the largest effectively nonlinear absorption coefficients (β) of 95.3 cm/GW among compounds **2**, **3** and **4** with the same conjugated length in their skeletons. In addition, the values of σ_e/σ_g and β of compound **2** are all larger than that of **4.** These results indicated that the electronic asymmetric property affected the nonlinear optical properties greatly. However, the values of σ_e/σ_g and β of the molecules with two electron withdrawing groups on both sides of their skeletons are much smaller than that of the molecules with two electron donor groups at both sides of their skeletons. The same conclusion could be concluded by comparison the values of σ_e/σ_g and β of **5** and **6** with **7** and **8**, respectively. These results are contrary to the calculated results of the first-order hyperpolarizabilities. The difference should be because that the selected calculation method is based on the absorption spectra of the title compounds, which are mainly dominated by the ground states of the molecules. While the nonlinear

Table 4
Calculated static β components and β ($\times 10^{-30}$ esu) values of the title compounds.

	β_{XXX}	β_{XYY}	β_{XZZ}	β_{YYY}	β_{XXY}	β_{YZZ}	β_{ZZZ}	β_{XXZ}	β_{YYZ}	β
1	−0.0008	−0.0001	0.0005	−0.0031	−0.0014	−0.0011	0.0022	0.0059	0.0002	0.00
2	−0.3627	−9.384	8.487	6.6439	3.742	−5.3117	14.62	−6.3315	4.9704	0.05
3	−1147.1	28.299	19.834	5.4501	59.86	1.2339	1.274	16.311	−2.543	4.06
4	−0.5679	−0.776	0.8967	0.089	0.543	−0.2672	1.673	102.909	1.2945	0.39
5	−188.98	2.129	−51.617	−26.761	253.05	−5.5823	15.31	−542.19	4.6943	2.27
6	−315.27	9.483	19.097	12.0371	−215.08	−9.0168	−9.99	364.16	−19.23	1.80
7	−149.48	11.552	4.650	3.7955	−17.45	−2.4531	11.48	33.904	−1.1253	0.52
8	−161.75	9.501	8.348	9.7556	−33.56	−10.644	−7.542	39.586	−16.406	0.55

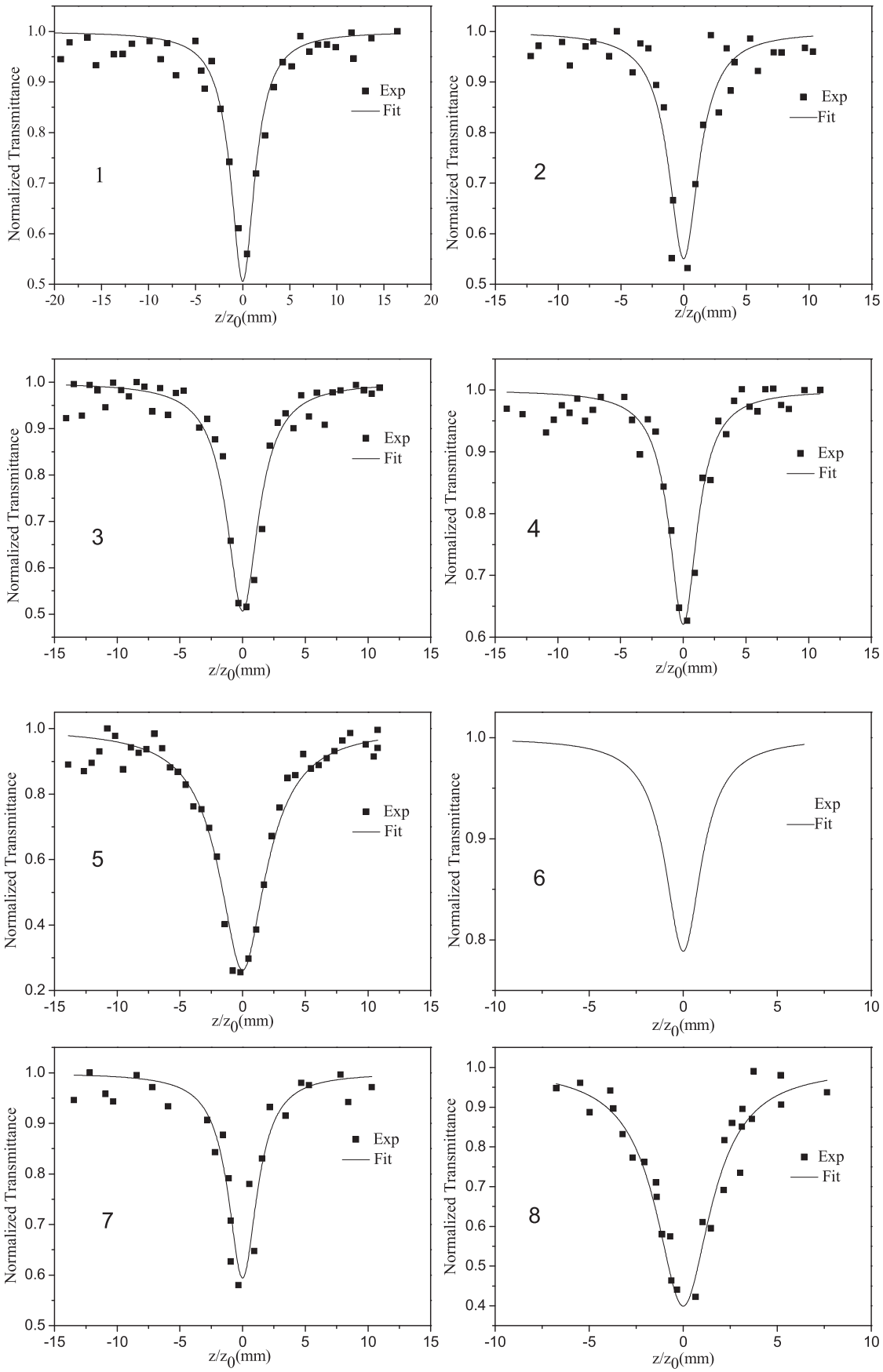

Fig. 5. Open aperture Z-scan traces of **1**–**8** in DMF solution.

Table 5
The absorption cross-sections of the ground state, the effective nonlinear absorption cross-sections and the effectively nonlinear absorption coefficients of platinum acetylides in DMF.

Compounds	$\sigma_g/10^{-18}cm^2$	$\sigma_e/10^{-18}$ cm^2	σ_e/σ_g	β(cm/GW)
1	0.90	1.68	1.86	9.03
2	1.90	4.10	2.15	46.5
3	2.50	7.72	3.10	95.3
4	2.01	2.14	1.06	21.3
5	3.70	4.51	1.21	100.1
6	1.25	1.95	1.56	45.74
7	3.33	12.4	3.72	248.1
8	1.45	12.8	8.82	110.8

absorption property, especially for the RSA, is mainly dominated by the excited states of the molecules. It can be seen from the data listed in Table 2 that the contributions of the Platinum atom to the electronic density of LUMO of **2, 7, 8** are much higher than that of **4, 5,** and **6**, respectively, relative to the contributions of the Platinum atom to electronic density of the HOMO of them. The large contributions of the heavy-atom to the electronic density of HOMO of a molecule, which is benefit to harvest triplet excited state, doesn't guarantee the better nonlinear absorption property.

The property of the triplet excited state plays more important role to the excited state absorption, especially for the nanosecond laser. The similar results also have been reported in the previous paper [45]. The values of σ_e/σ_g and β of **5** are 1.14 and 4.70 times larger than those of **4**, respectively, and the values of σ_e/σ_g and β of **7** are 1.73 and 5.34 times larger than those of **2**. The results inferred that the nonlinear absorption properties of a molecule can be enhanced by enlarging the conjugate length of the molecule, which is coincident with the calculation results. It is notable that the values of β of **5** and **7** are larger than those of **6** and **8**, but the values of σ_e/σ_g of **5** and **7** are smaller than those of **6** and **8**, respectively. These results indicated that enlarging the conjugated area in the center of the molecule was disadvantageous to the nonlinear absorption property of the molecule, which maybe because of the large contributions of the naphthalene to the electronic density of HOMO and LUMO of the molecules as listed in Table 2.

4. Conclusion

In summary, the relationship between the structure and the nonlinear absorption property of the platinum(II) acetylides via computational method and experiments was investigated detailedly. The time-dependent functional theory (TD-DFT) method with exchange correlation function B3LYP, which was selected by comparison the calculated electronic absorption spectra with the experimental absorption spectra of the Platinum acetylides, was used to calculate the properties of the ground and excited states them, and then the first-order hyperpolarizabilities were calculated out based on the calculated properties of the ground and excited of them. The Z-scan results indicated that the electronic asymmetric property is the most important factor affected the nonlinear optical properties, and the nonlinear absorption properties of a molecule can be enhanced by enlarging the conjugate length of the molecule. The nonlinear optical property of the molecules with two electron donor groups at both sides of their skeletons are better than that of the molecules with two electron withdrawing groups. Enlarging the conjugated area in the center of the molecule was disadvantageous to the nonlinear absorption property of the molecule, and the large contribution of the heavy-atom to the electronic density of HOMO of a molecule doesn't mean the better nonlinear absorption property. The large values of σ_e/σ_g and the short fluorescence lifetimes of the complexes infer that the nonlinear absorption behavior of the titles complexes should be originated reverse saturable absorption. Most of the calculated results are consistent with the Z-scan results, the deviation of the calculated results from the Z-scan results should be because that the calculation method is selected based on the absorption spectra of the title compounds, which are mainly dominated by the ground states of the molecules. However, the nonlinear absorption property is mainly dominated by the excited states of the molecules.

Declaration of competing interest

The authors declare that they have no known competing financial interests or personal relationships that could have appeared to influence the work reported in this paper.

Appendix A. Supplementary data

Supplementary data to this article can be found online at https://doi.org/10.1016/j.jorganchem.2019.121003.

References

[1] G. He, L. Tan, Q. Zheng, P. Prasad, Chem. Rev. 108 (2008) 1245–1330.
[2] K. Belfield, S. Yao, M. Bondar, Adv. Polym. Sci. 213 (2008) 97–156.
[3] S. Charan, B.G. Bharate, Inorg. Chim. Acta 394 (2013) 598–604.
[4] F. Dai, H. Zhan, Q. Liu, Y. Fu, J. Li, Q. Wang, Z. Xie, L. Wang, F. Yan, W. Wong, Chem. Eur J. 18 (2012) 1502–1511.
[5] Y. Wu, T. Sasaki, S. Nakai, A. Yokotani, H. Tang, Appl. Phys. Lett. 62 (1993) 2614–2615.
[6] F. Liang, L. Kang, Z. Lin, Y. Wu, Cryst. Growth Des. 17 (2017) 2254–2289.
[7] P. Ray, Chem. Rev. 110 (2010) 5332–5365.
[8] B. Sahraoui, R. Czaplicki, A. Klöpperpieper, A. Andrushchak, A. Kityk, J. Appl. Phys. 107 (2010), 113526.
[9] A. Rad, K. Ayub, Comput. Theor. Chem 1121 (2017) 68–75.
[10] J. Wessels, H. Nothofer, W. Ford, A. Vossmeyer, J. Am. Chem. Soc. 126 (2004) 3349–3356.
[11] S. Zheng, A. Leclercq, J. Fu, L. Beverina, Chem. Mater. 19 (2007) 432–442.
[12] Y. Chen, L. Gao, M. Feng, L. Gu, N. He, J. Wang, Y. Araki, W.J. Blau, O. Ito, Mini-Reviews Org. Chem. 6 (2009) 55–65.
[13] Y. Chen, S. O'Flaherty, M. Fujitsuka, M. Hanack, L.R. Subramanian, O. Ito, W.J. Blau, Chem. Mater. 14 (2002) 5163–5168.
[14] F. Guo, W. Sun, Y. Liu, K. Schanze, Inorg. Chem. 44 (2005) 4055–4065.
[15] A. Shelton, R. Price, L. Brokmann, B. Dettlaff, K. Shanze, Appl. Mater. Interfaces. 5 (2013) 7867–7874.
[16] M. Bruce, J. Davy, B. Hall, Y. Galen, B. Skelton, A. White, Appl. Organomet. Chem. 16 (2002) 559–568.
[17] T. Cooper, D. Krein, A. Burke, D. Mclean, J. Haley, J. Slagle, J. Monahan, A. Fratiti, J. Phys. Chem. A 116 (2012) 139–149.
[18] C. Powell, M. Cifuentes, J. Morral, R. Stranger, M. Humphrey, M. Samoc, B. Luther Davies, G. Heath, J. Am. Chem. Soc. 125 (2003) 602–610.
[19] J. Zhao, W. Wu, J. Sun, S. Guo, Chem. Soc. Rev. 42 (2013) 5323–5351.
[20] G. Zhou, W. Wong, Chem. Soc. Rev. 40 (2011) 2541–2566.
[21] P. Xie, L. Wang, Z. Huang, F. Guo, Q. Jin, Eur. J. Inorg. Chem. 28 (2014) 2544–2551.
[22] G. Zhou, W. Wong, D. Cui, C. Ye, Chem. Mater. 17 (2005) 5209–5217.
[23] J.E. Rogers, J.E. Slagle, D.M. Krein, A.R. Burke, B.C. Hall, A. Fratini, D.G. McLean, P.A. Fleitz, T.M. Cooper, M. Drobizhev, N.S. Makarov, A. Rebane, K.Y. Kim, R. Farley, K.S. Schanze, Inorg. Chem. 46 (2007) 6483–6494.
[24] Y. Chen, L. Gao, M. Feng, L. Gu, N. He, J. Wang, Y. Araki, W. Blau, O. Ito, Mini-Reviews Org. Chem. 6 (2009) 55–65.
[25] E. Glimsdal, M. Carlsson, T. Kindahl, M. Lindren, C. Lopes, B. Eliasson, J. Phys. Chem. A 114 (2010) 3431–3442.
[26] D. Yao, H. Wang, L. Zhang, F. Guo, J. Organomet. Chem. 752 (2014) 6–11.
[27] S. Hassan, F. Nawaz, Z. Khan, A. Firdous, M. Farid, M. Nazir, Opt. Mater. 86 (2018) 106–112.
[28] M. Sheik-bahae, A. Said, T. Wei, D. Hagan, E. Stryland, IEEE J. Quantum Electron. 26 (1990) 760–767.
[29] M. Sheik-bahae, A. Said, E. Stryland, Opt. Lett. 14 (1989) 955–957.
[30] P. Chapple, J. Staromlynska, J. Hermann, T. Mckay, R. Mcduff, J. Nonlinear Opt. Phys. Mater. 6 (1997) 251–293.
[31] M. Bharati, S. Bhattacharya, J. Suman Krishna, L. Giribabu, S. Venugopal Rao, Opt. Laser. Technol. 108 (2018) 418–425.
[32] M.J. Frisch, G.W. Trucks, H.B. Schlegel, G.E. Scuseria, M.A. Robb, J.R. Cheeseman, G. Scalmani, V. Barone, B. Mennucci, G.A. Petersson, H. Nakatsuji, M. Caricato, X. Li, H.P. Hratchian, A.F. Izmaylov, J. Bloino, G. Zheng, J.L. Sonnenberg, M. Hada, M. Ehara, K. Toyota, R. Fukuda, J. Hasegawa, M. Ishida, T. Nakajima, Y. Honda, O. Kitao, H. Nakai, T. Vreven, J.A. Montgomery Jr., J.E. Peralta, F. Ogliaro, M. Bearpark, J.J. Heyd, E. Brothers,

K.N. Kudin, V.N. Staroverov, T. Keith, R. Kobayashi, J. Normand, K. Raghavachari, A. Rendell, J.C. Burant, S.S. Iyengar, J. Tomasi, M. Cossi, N. Rega, J.M. Millam, M. Klene, J.E. Knox, J.B. Cross, V. Bakken, C. Adamo, J. Jaramillo, R. Gomperts, R.E. Stratmann, O. Yazyev, A.J. Austin, R. Cammi, C. Pomelli, J.W. Ochterski, R.L. Martin, K. Morokuma, V.G. Zakrzewski, G.A. Voth, P. Salvador, J.J. Dannenberg, S. Dapprich, A.D. Daniels, O. Farkas, J.B. Foresman, J.V. Ortiz, J. Cioslowski, D.J. Fox, Gaussian, Inc., Wallingford CT, 2013.
[33] J. Yang, Q. Zhu, J. Chem. Phys. 118 (2003) 9608–9613.
[34] A. Becke, J. Chem. Phys. 98 (1993) 1372–1377.
[35] P.J. Hay, W. Wadt, J. Chem. Phys. 82 (1985) 270–283.
[36] P.J. Hay, W. Wadt, J. Chem. Phys. 82 (1985) 299–310.
[37] Y. Zhu, Z. Chen, Z. Guo, J. Mol. Model. 15 (2009) 469–479.
[38] N.M. O'Boyle, J.G. Vos, GaussSum 2.0, Dublin City University, 2006.
[39] N. Ma, S. Sun, C. Liu, X. Sun, J. Phys. Chem. A 115 (2011) 13564–13572.
[40] S. Muthu, E.I. Paulraj, Solid State Sci. 14 (2012) 476–487.
[41] F. Huyskens, P. Huyskens, A. Person, J. Chem. Phys. 108 (1998) 8161–8171.
[42] E. Donmez, H. Kara, A. Karakas, Spectrochim. Acta, Part A 66 (2007) 1141–1146.
[43] D. Kanis, M. Ratner, T. Marks, Chem. Rev. 94 (1994) 195–242.
[44] G. Wood, M. Miller, A. Mott, Opt. Lett. 20 (1995) 973–975.
[45] G. Zhou, W. Wong, S. Pong, C. Ye, Z. Lin, Adv. Funct. Mater. 19 (2009) 531–544.